Reachable Eigenanalysis

Yifan Zhou, *Member, IEEE*, and Peng Zhang, *Senior Member, IEEE*

***Abstract*—This letter devises a Reachable Eigenanalysis (*ReachEigen*) theory as a formal method to analyze uncertain eigenvalues in power systems. *ReachEigen* computes the set of the possible spectra, taking into account the changes of both the system operating points and the characteristic equations caused by uncertainties. The innovation of *ReachEigen* lies in: 1) a Newton-iteration-based eigensolver which tractably tackles the "random walk" of steady-state operating points and delineates the propagation of uncertainty effects in the system eigenvalues; and 2) a reachability method established on the Netwon's eigensolver, which bounds the set of uncertain eigenvalues through a single calculation and thus is immune to the combinatorial explosion issue under a large number of uncertain factors. Case studies on a networked microgrid verifies the efficiency of *ReachEigen* and its superiority over existing methods. The efficacy of *ReachEigen* of providing early warning information for small-signal stability under uncertainties is also illustrated.**

***Index Terms*—Reachable eigenanalysis, formal method, uncertainty, small-signal stability, networked microgrid.**

I. Introduction

EIGENANALYS, although indispensable for quantifying the nature of instability and tuning controls for mitigating oscillations, has become an intractable problem for today's power grids penetrated with uncertain distributed energy resource (DERs) [1]. The main challenges arise from: 1) the uncertainties propel the system to new operating points; 2) the uncertainties and shifted operating points conjointly perturb the characteristic equations. So far, there is a lack of uncertain eigenanalysis approaches to computing the uncertain eigenvalues as well as addressing the aforementioned uncertainty impacts. Simulation-based methods such as Monte Carlo algorithms [2], [3] fail to enumerate the infinitely many uncertain scenarios. Analytical methods such as perturbation theory [4], Gershgorin circle [5], and interval eigenvalue [6] rely largely on the Taylor expansion of the state matrix, which completely neglect the 'random walk' of the operating points disturbed by uncertainties and unavoidably lead to incorrect uncertain eigenvalue results. Failing to capture all possible eigenvalue results, those non-formal eigenanalysis methods could engender overly optimistic operation decisions potentially leading to catastrophic consequences.

Manuscript received February 29, 2020; revised June 4, 2020; accepted July 10, 2020. Date of publication July 20, 2020; date of current version November 4, 2020. This work was supported in part by the National Science Foundation under Grant ECCS-1831811 and in part by the Department of Energy's Advanced Grid Modeling Program. Paper no. PESL-00058-2020. *(Corresponding author: Peng Zhang.)*

The authors are with the Department of Electrical and Computer Engineering, Stony Brook University, Stony Brook, NY 11794 USA (e-mail: yifan.zhou.1@stonybrook.edu; p.zhang@stonybrook.edu).

Color versions of one or more of the figures in this article are available online at https://ieeexplore.ieee.org.

Digital Object Identifier 10.1109/TPWRS.2020.3009860

To tackle the challenges, this letter devises Reachable Eigenanalysis (*ReachEigen*), an analytical and formal method which computes the reachable spectra under uncertainties. The salient features of *ReachEigen* lie in its resolution of incorporating the shifting operating points caused by uncertainties and its capability of finding the eigenvalue sets in a single computation. *ReachEigen* therefore opens a door of new approaches to predicting and mitigating the hazardous stability issues in modern power systems.

II. Eigensolver Based on Virtual ODE Integral

A. Uncertain Eigenanalysis Basics

A dynamical power system subject to uncertain inputs $\boldsymbol{u}$ can be described by the following differential-algebraic system of equations (DAEs):

$$\dot{\boldsymbol{x}}_d(t) = \boldsymbol{f}_d(\boldsymbol{x}_d, \boldsymbol{x}_a, \boldsymbol{u}), \quad \boldsymbol{0} = \boldsymbol{f}_a(\boldsymbol{x}_d, \boldsymbol{x}_a, \boldsymbol{u}) \tag{1}$$

where $\boldsymbol{x}_d$ and $\boldsymbol{x}_a$ respectively denote the differential/algebraic variables; $\boldsymbol{f}_d$ and $\boldsymbol{f}_a$ formulate the system functions. In this letter, we focus on the unknown-but-bounded $\boldsymbol{u}$ which can be modeled by a set. The uncertain eigenanalysis under a specified $\boldsymbol{u}$ should be performed in two steps:

1) Solve the equilibrium point stimulated by $\boldsymbol{u}$, i.e., $\boldsymbol{x}^{(u)} = [\boldsymbol{x}_d^{(u)}; \boldsymbol{x}_a^{(u)}]$, by the steady-state equations of (1).
2) Construct the state matrix $\boldsymbol{A}$ with $\boldsymbol{x}^{(u)}$ and $\boldsymbol{u}$ through $\Delta\dot{\boldsymbol{x}}(t) = \boldsymbol{A}\Delta\boldsymbol{x}$ and compute the eigenvalues $\lambda^{(u)}$ by:

$$|\boldsymbol{A} - \lambda^{(u)}\boldsymbol{I}| = 0 \tag{2}$$

where $\Delta\boldsymbol{x}$ denotes the deviation of $\boldsymbol{x}_d$, $\boldsymbol{I}$ is the identity matrix.

B. Ordinary Differential Equations (ODEs) Based Eigensolver

This subsection devises a Newton-based eigensolver to compute the k^{th} eigenvalue of (2), denoted as $\lambda_k = \lambda_{r,k} + j\lambda_{i,k}$. The prerequisite of this new solver is the eigen-result of the deterministic case, i.e., $\lambda_k^{(0)}$ as the k^{th} eigenvalue and $\boldsymbol{\psi}_k^{(0)} = \boldsymbol{\psi}_{r,k}^{(0)} + j\boldsymbol{\psi}_{i,k}^{(0)}$ as its left eigenvector. For brevity, the subscript k is omitted in the following.

When there exists uncertainty $\boldsymbol{u}$, the steady-state equations of (1) are required to solve the new equilibrium point $\boldsymbol{x}^{(u)}$ with respect to $\boldsymbol{u}$:

$$\boldsymbol{f}_d(\boldsymbol{x}_d^{(u)}, \boldsymbol{x}_a^{(u)}, \boldsymbol{u}) = \boldsymbol{0}, \quad \boldsymbol{f}_a(\boldsymbol{x}_d^{(u)}, \boldsymbol{x}_a^{(u)}, \boldsymbol{u}) = \boldsymbol{0} \tag{3}$$

The next step is to construct the characteristic equation $\boldsymbol{A\phi} = \lambda\boldsymbol{\phi}$, where $\boldsymbol{A}$ is a function of both $\boldsymbol{x}^{(u)}$ and $\boldsymbol{u}$. By separating it into real and imaginary parts, we can obtain

$$\boldsymbol{A\phi}_r = \lambda_r\boldsymbol{\phi}_r - \lambda_i\boldsymbol{\phi}_i, \quad \boldsymbol{A\phi}_i = \lambda_r\boldsymbol{\phi}_i + \lambda_i\boldsymbol{\phi}_r \tag{4}$$

where $\boldsymbol{\phi} = \boldsymbol{\phi}_r + j\boldsymbol{\phi}_i$ denotes the right eigenvector of λ.

Further, to ensure a unique eigenvector solution of (4), constraint $\boldsymbol{\psi}^{(0)}\boldsymbol{\phi} = 1$ is introduced,[1] which yields the following:

$$\boldsymbol{\psi}_r^{(0)}\boldsymbol{\phi}_r - \boldsymbol{\psi}_i^{(0)}\boldsymbol{\phi}_i = 1, \;\; \boldsymbol{\psi}_r^{(0)}\boldsymbol{\phi}_i + \boldsymbol{\psi}_i^{(0)}\boldsymbol{\phi}_r = 0 \tag{5}$$

Equations (3)–(5) collectively determine the uncertain eigenvalues. Denoting $\boldsymbol{y} = [\lambda_r; \lambda_i; \boldsymbol{\phi}_r; \boldsymbol{\phi}_i; \boldsymbol{x}_d^{(u)}; \boldsymbol{x}_a^{(u)}]$, (3)–(5) can be abstracted as $\boldsymbol{g}(\boldsymbol{y}, \boldsymbol{u}) = 0$, which can be solved by Newton's method to acquire $\boldsymbol{y}$ numerically:

$$\boldsymbol{y}_{n+1} = \boldsymbol{y}_n - (\boldsymbol{J}_g(\boldsymbol{y}_n, \boldsymbol{u}))^{-1}\boldsymbol{g}(\boldsymbol{y}_n, \boldsymbol{u}) \tag{6}$$

where $\boldsymbol{y}_n$ is the value of $\boldsymbol{y}$ at the n^{th} iteration; $\boldsymbol{J}_g = \partial \boldsymbol{g}/\boldsymbol{y}|_{\boldsymbol{y}=\boldsymbol{y}_n}$ denotes the Jacobian matrix of $\boldsymbol{g}$ at point $\boldsymbol{y}_n$.

The discrete equations in (6) are deemed an abstraction of a continuous dynamics, viz. an ODE-Eigen model, as follows:

$$\begin{cases} \dot{\boldsymbol{y}}(t) = -(\boldsymbol{J}_g(\boldsymbol{y}, \boldsymbol{u}))^{-1}\boldsymbol{g}(\boldsymbol{y}, \boldsymbol{u}) & \text{(7a)} \\ \dot{\boldsymbol{u}}(t) = 0 & \text{(7b)} \end{cases}$$

where (7a) formulates the continuous dynamic of (6); (7b) indicates that $\boldsymbol{u}$ does not change during a single eigenanalysis.

The ODE-Eigen model in (7) enables analyzing the uncertain impact of a set of $\boldsymbol{u}$ by integrals of those ODEs because the integration process accurately reflects how the uncertainty from $\boldsymbol{u}$ propagates into the system eigenvalues.

III. Reachable Eigenanalysis

A. ReachEigen *Formulation*

The ODE-Eigen model in (7) is further abstracted by:

$$\dot{\boldsymbol{z}}(t) = \boldsymbol{h}(\boldsymbol{z}(t)) \tag{8}$$

where $\boldsymbol{z} = [\boldsymbol{y}; \boldsymbol{u}]$; $\boldsymbol{h}(\boldsymbol{z}) = [\boldsymbol{h}_y(\boldsymbol{y}, \boldsymbol{u}); \boldsymbol{h}_u(\boldsymbol{y}, \boldsymbol{u})]$; $\boldsymbol{h}_y = -(\boldsymbol{J}_g(\boldsymbol{y}, \boldsymbol{u}))^{-1}\boldsymbol{g}(\boldsymbol{y}, \boldsymbol{u})$; $\boldsymbol{h}_u = \boldsymbol{0}$.

Given $\mathcal{U}^0$ as the set of uncertainty inputs modelled by a zonotope, finding the set of the k^{th} eigenvalue is formulated as the reachable eigenvalue (*ReachEigen*) set defined as:

$$\mathcal{R}_{eig} = \left\{ \boldsymbol{z} = \int_0^\infty \boldsymbol{h}(\boldsymbol{z}(\tau))d\tau \;\middle|\; \boldsymbol{y}(0) \in \mathcal{Y}^0, \boldsymbol{u} \in \mathcal{U}^0 \right\} \tag{9}$$

where $\mathcal{Y}^0 = \{[\lambda_r^{(0)}; \lambda_i^{(0)}; \boldsymbol{\phi}_r^{(0)}; \boldsymbol{\phi}_i^{(0)}; \boldsymbol{x}_d^{(0)}; \boldsymbol{x}_a^{(0)}]\}$ denotes the initial point for ODE integral.

Define the reachable set of (8) at time point t as:

$$\mathcal{R}(t) = \left\{ \boldsymbol{z}(t) = \int_0^t \boldsymbol{h}(\boldsymbol{z}(\tau))d\tau \;\middle|\; z(0) \in \mathcal{Z}^0 \right\} \tag{10}$$

where $\mathcal{Z}^0 = \mathcal{Y}^0 \otimes \mathcal{U}^0$; $\otimes$ denotes the Cartesian product. Further, the reachable set during time interval $[k\Delta t, (k+1)\Delta t]$ is defined as the union of time-point reahcable sets:

$$\mathcal{R}([k\Delta t, (k+1)\Delta t]) = \cup_{t \in [k\Delta t, (k+1)\Delta t]} \mathcal{R}(t) \triangleq \mathcal{R}_k \tag{11}$$

Upon the local linearization of (8), $\mathcal{R}(t)$ can be over-approximated by a reachable set of the linear abstraction $\mathcal{R}^{lin}(t)$ and the second-order error $\mathcal{R}^{err}(t)$[7]:

$$\mathcal{R}(t) \subseteq \mathcal{R}^{lin}(t) \oplus \mathcal{R}^{err}(t) \tag{12}$$

Here, $\oplus$ denotes the Minkowski addition; $\mathcal{R}^{err}(t)$ is the error due to the Lagrange remainder [7]; $\mathcal{R}^{lin}(t)$ is the reachable set of the linear abstraction of (8), which is computed as:

$$\begin{aligned} \mathcal{R}^{lin}(t) = & \left(e^{\boldsymbol{B}\Delta t}(\mathcal{R}(t-\Delta t) - \boldsymbol{z}^{lin})\right) \\ & \oplus \left(\boldsymbol{B}^{-1}(e^{\boldsymbol{B}\Delta t} - \boldsymbol{I})\boldsymbol{h}(\boldsymbol{z}^{lin})\right) \oplus \boldsymbol{z}^{lin} \end{aligned} \tag{13}$$

where $\boldsymbol{z}^{lin}$ denotes the linearization point; $\boldsymbol{B}$ denotes the jacobian matrix of $\boldsymbol{h}$ at $\boldsymbol{z}^{lin}$.

B. ReachEigen *Algorithm*

Based on the formulation in Subsection III-A, Fig. 1 presents the overall procedure of the *ReachEigen* algorithm. The superiority of *ReachEigen* is three-fold: (i) the validity of *ReachEigen* is theoretically ensured by the reachability theory, which over-approximates the uncertain eigenvalues under $\mathcal{U}^0$; (ii) *ReachEigen* is an inherently analytical algorithm allowing the computation of the set of uncertain eigenvalues in a single run, which makes the random sampling process unnecessary. (iii) *ReachEigen* addresses the "random walk" of the power system operating points in eigenanalysis via the ODE-Eigen model, which incorporates both the steady state Equation (3) and the state matrix (4) and thus take into account the effect of both both $\boldsymbol{x}^{(u)}$ and $\boldsymbol{u}$.

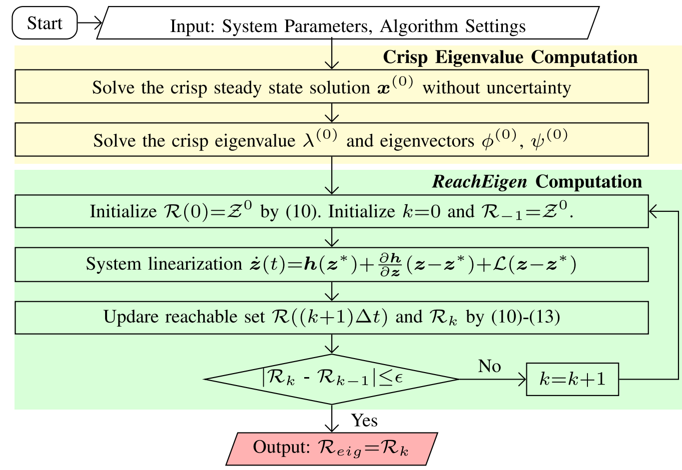

Fig. 1. Overall algorithm flowchart of *ReachEigen*.

IV. Case Study

ReachEigen is verified on a networked microgrid system composed of three microgrids. Each microgrid is powered by 3 DERs equipped with droop controllers [8]. The crisp eigenvalue spectrum for the microgrid without uncertainties is illustrated in Fig. 2. The *ReachEigen* algorithm is implemented in MATLAB R2019b on a 2.50 GHz PC.

[1]Equation (5) is reasonable because for any eigenvector solution $\boldsymbol{v}$ from (4), its multiplication with a non-zero number is still an eigenvector. Hence, $\boldsymbol{\psi}^{(0)}\boldsymbol{v}$ can be rotated and scaled by a complex number $\mu e^{j\theta}$ to satisfy $1 = \mu e^{j\theta}(\boldsymbol{\psi}^{(0)}\boldsymbol{v}) = \boldsymbol{\psi}^{(0)}(\mu e^{j\theta}\boldsymbol{v})$ as long as $\boldsymbol{\psi}^{(0)}\boldsymbol{v} \neq 0$.

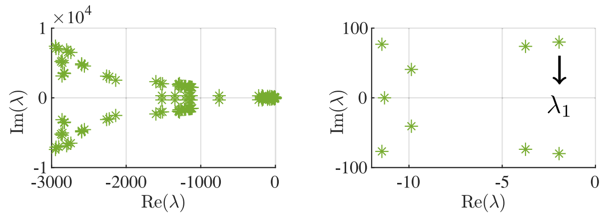

(a) Complete eigenvalue spectrum (b) Low-frequency eigenvalues

Fig. 2. Eigenvalue spectrum of the deterministic case.

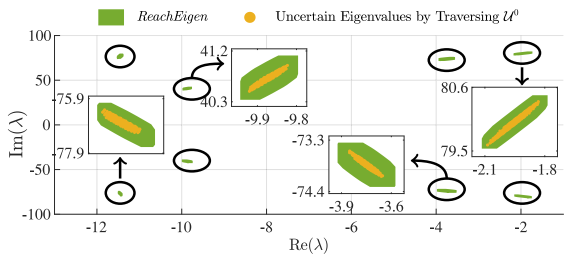

Fig. 3. *ReachEigen* spectrum (low-frequency modes) under 20% uncertainty.

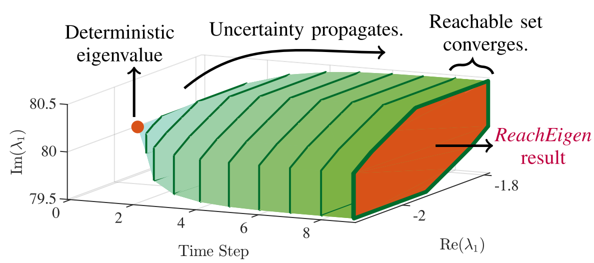

Fig. 4. Computational process of *ReachEigen*.

A. *Validity of* ReachEigen

This subsection verifies the validity of *ReachEigen*. Figure 3 illustrates the *ReachEigen* spectrum of the low-frequency modes, with 20% uncertainty from the generation of each DER. Rather than the crisp eigenvalues shown in Fig. 2, *ReachEigen* delineates the zonotopes of possible eigenvalues under specific uncertainties, as shown in the zoomed-in subplots in Fig. 3. Eigenvalue solutions by traversing the uncertainty space $\mathcal{U}^0$ via 20,000 Monte Carlo runs assumably provide the actual uncertain eigenvalue set (see the yellow dots) to verify that *ReachEigen* (shown in the green region) is able to cover the uncertain eigenvalues.

Fig. 4 visualizes the computing process of *ReachEigen*. Starting from the crisp eigen-result, the reachable set of eigenvalues continues to update itself along with the ODE-Eigen dynamics which is a numerical replica of the propagation of the uncertainty impact. It can be seen that the reachable eigenvalues are obtained after *ReachEigen* converges in 10 iterations.

Table I presents the computational efficiency of *ReachEigen* for both a single microgrid and the networked microgrids and a comparison with Monte Carlo sampling. Denote n as the system dimension and n_u as the number of uncertainty factors. Theoretically, performing Monte Carlo-based eigenanalyses by traversing the uncertainty space leads to a computational complexity of $o(p^{n_u}) \times o(n^2) \sim o(p^{n_u}) \times o(n^3)$ (here, p is the sampling number of each dimension of $\boldsymbol{u}$), while the worst complexity of *ReachEigen* is $o((3n + n_u + 2)^5)$ according to the reachability analysis theory [7].

TABLE I
COMPUTING TIME OF *REACHEIGEN*

Test system	*ReachEigen*	Monte Carlo (20,000 runs)
3-DER microgrid [8]	20.33s	68.95s
9-DER networked microgrid	120.25s	276.08s

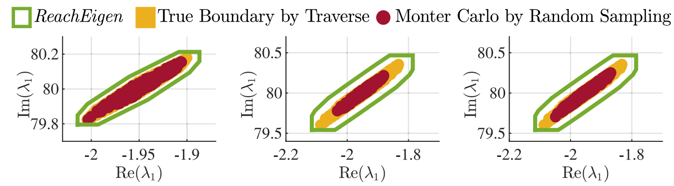

(a) $n_u = 3$; 500 samples (b) $n_u = 9$; 500 samples (c) $n_u = 9$; 10000 samples

Fig. 5. *ReachEigen* v.s. Monte Carlo method.

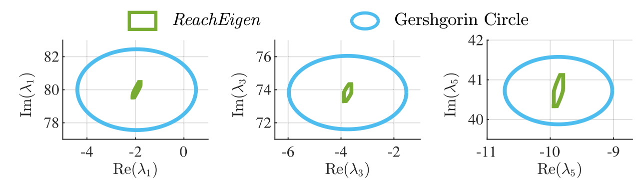

(a) Set of λ_1 (b) Set of λ_3 (c) Set of λ_5

Fig. 6. *ReachEigen* v.s. Gershgorin circle method.

B. *Comparison With Existing Methods*

This subsection compares *ReachEigen* with the Monte Carlo method [2] and the Gershgorin circle method [5], i.e., representatives of simulation-based methods and analytical methods respectively.

Fig. 5 compares *ReachEigen* with Monte Carlo method. With small n_u (i.e., number of uncertainty factors), randomized Monte Carlo sampling yields reasonable results, as illustrated by Fig. 5(a). When n_u is large, however, most of the extreme scenarios are missed, as revealed by Fig. 5(b)-(c); even worse, increasing the number of Monte Carlo samples does not help fix this defect. This overly optimistic indicators will induce severe operational hazards.

Fig. 6 compares *ReachEigen* with the Gershgorin circle method. Combined with the quasi-diagonalization technique [5], the Gershgorin circles can be effectively tightened. However, it is obvious that the Gershgorin circles (i.e., the blue circles) still lead to excessively conservative results. In contrast, *ReachEigen* is more accurate benefiting from the tightness of the zonotope-based reachability analysis.

Moreover, *ReachEigen* addresses the impact of "random walks" of steady-state operating points, which is overlooked by existing analytical methods. When disturbed by uncertainties, the power system transitions to new steady-state operating points, which impacts the small-signal stability of the power system together with the uncertain inputs. Fig. 7 illustrates that

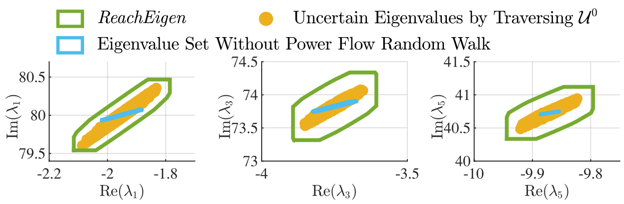

(a) Set of λ_1 (b) Set of λ_3 (c) Set of λ_5

Fig. 7. Impact of operating point "random walk" on uncertain eigenvalues.

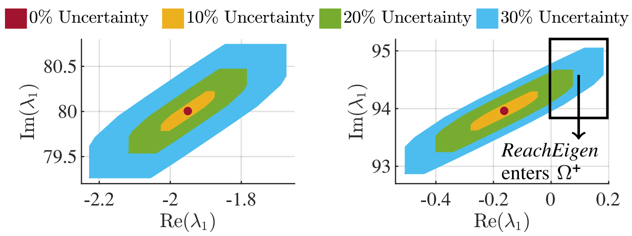

(a) $m_p = 0.3\%, n_q = 3\%$ (b) $m_p = 0.38\%, n_q = 4\%$

Fig. 8. Networked microgrid small-signal stability via *ReachEigen* analysis: (a) stable case; (b) early-warning alarm triggered at 20% uncertainty and beyond.

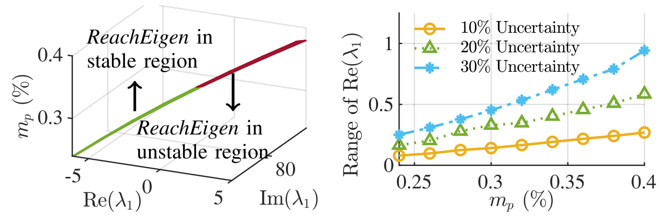

(a) *ReachEigen* trajectory (b) Range of $\mathrm{Re}(\lambda_1)$

Fig. 9. Impact of P-f droop control gain on *ReachEigen*.

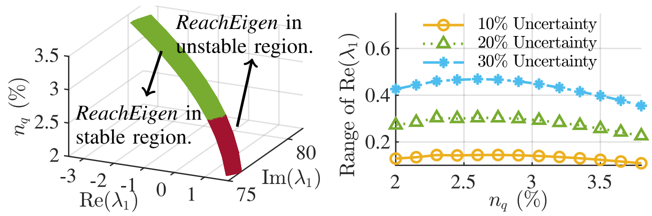

(a) *ReachEigen* trajectory (b) Range of $\mathrm{Re}(\lambda_1)$

Fig. 10. Impact of Q-V droop control gain on *ReachEigen*.

without considering this "random walk" effect, the uncertain eigenvalue assessment will be severely over-optimistic, leading to significant hazards in power system operation.

C. Efficacy of ReachEigen

This subsection explores the efficacy of *ReachEigen* in providing the early-warning information for the small-signal stability of networked microgrids via the *ReachEigen* of the rightmost eigenvalue (i.e., λ_1 as pointed in Fig. 2(b)).

Fig. 8 illustrates the expansion of *ReachEigen* of λ_1 with the increasing uncertainty from each DER. Two sets of the droop parameters are studied. Here, m_p denotes the P-f droop control gain and n_q denotes the Q-V droop control gain:

$$\Delta\omega = -m_p \Delta P, \quad \Delta V = -n_q \Delta Q \tag{14}$$

where ω, V, P, Q respectively represent the angular frequency, voltage, active power and reactive power.

In any of the four cases, the deterministic eigenvalue marked by the red dots indicates a stable operating point of the networked microgrid, as shown in Fig. 8. Whereas, *ReachEigen* is able to reveal hidden hazards which cannot be captured by the deterministic eigenanalysis. In Fig. 8(a), *ReachEigen* indicates that the small-signal stability is always guaranteed even with a 30% uncertainty; however, in Fig. 8(b), *ReachEigen* under 20% uncertainty enters the right half-plane, which clearly reveals the risk of unstable equilibrium points caused by the DER uncertainties.

Further, Figs. 9 and 10 illustrate the impact of droop control gains on *ReachEigen*. With the increase of m_p, *ReachEigen* expands and moves towards the right half-plane, indicating the tendency in the networked microgrid to have unstable equilibrium points as well increased vulnerabilities to uncertainties. In contrast, the increase of n_q leads to an improved small-signal stability and strengthened robustness of the networked microgrid.

V. Conclusion

This letter introduces a Reachable Eigenanalysis (*ReachEigen*) method for analytically estimating the impact of uncertainties on the power system eigenvalues. As a formal method, *ReachEigen* over-approximates the uncertain eigenvalues perturbed by both the uncertainties and the "random walk" of the operating points. Case studies show the efficacy of *ReachEigen* to formally verify the power system small-signal stability under various uncertainties. The next step is to develop a distributed *ReachEigen* and incorporate probabilistic distributions and dependencies in *ReachEigen*.

References

[1] R. Majumder, "Some aspects of stability in microgrids," *IEEE Trans. Power Syst.*, vol. 28, no. 3, pp. 3243–3252, Aug. 2013.

[2] H. Huang, C. Chung, K. W. Chan, and H. Chen, "Quasi-Monte Carlo based probabilistic small signal stability analysis for power systems with plug-in electric vehicle and wind power integration," *IEEE Trans. Power Syst.*, vol. 28, no. 3, pp. 3335–3343, Aug. 2013.

[3] A. U. Krismanto, N. Mithulananthan, and I. Kamwa, "Oscillatory stability assessment of microgrid in autonomous operation with uncertainties," *IET Renewable Power Gener.*, vol. 12, no. 4, pp. 494–504, 2017.

[4] Y. Zhu, C. Liu, and L. Yao, "A faster estimation method for electromechanical oscillation frequencies," *IEEE Trans. Power Syst.*, vol. 34, no. 4, pp. 3280–3282, Jul. 2019.

[5] Y. Li, P. Zhang, L. Ren, and T. Orekan, "A Geršgorin theory for robust microgrid stability analysis," in *Proc. IEEE Power Energy Soc. General Meeting*, 2016, pp. 1–5.

[6] J. Ma, T. Wang, Z. Wang, and J. S. Thorp, "Interval Eigenvalue analysis of closed-loop control for power system oscillation with interval parameters," in *Proc. IEEE Power Energy Soc. General Meeting*, 2012, pp. 1–6.

[7] B. Schürmann, N. Kochdumper, and M. Althoff, "Reachset model predictive control for disturbed nonlinear systems," in *Proc. IEEE Conf. Decis. Control*, 2018, pp. 3463–3470.

[8] N. Pogaku, M. Prodanovic, and T. C. Green, "Modeling, analysis and testing of autonomous operation of an inverter-based microgrid," *IEEE Trans. Power Electron.*, vol. 22, no. 2, pp. 613–625, Mar. 2007.